Title:
Spiral Paths for Pocket Machining with Limited Tool Engagement Angle

Authors:
Martin Held, held@cs.sbg.ac.at, Universität Salzburg
Josef Pfeiffer, jpfeiffer@cs.sbg.ac.at, Universität Salzburg

Keywords:
Pocket Machining, Tool Engagement Angle, Cutting Width, Spiral, Voronoi Diagram, Medial Axis

DOI: 10.14733/cadconfP.2026.106-111

Introduction:

Pocket machining is a material-removal process used to create an internal cavity within a workpiece. In order to cope with the requirements of high-speed machining (HSM), recent pocketing approaches try to achieve smooth paths by applying trochoidal or spiral-like patterns. E.g., Elber et al. [1] use Voronoi diagrams to place locally maximal-sized disks inside the pocket and link those disks to trochoidal paths.

In addition to achieving smooth paths, successful high-speed pocketing also requires control of important cutting parameters. The *engagement angle* at a point T on the tool path represents the contact angle between the material and the tool centered at T, see Figure 1a. It is determined by the point L on the tool circle that lies on a line through T that is perpendicular to the tangent of the tool trajectory at T. The second important point is the point E where the tool enters the area not yet machined. The *cutting width* corresponds to the depth that the tool cuts material along a radial direction perpendicular to the trajectory of the tool, see Figure 1b. The tool engagement angle is known to be a decent proxy for the forces acting on the tool. However, the tool engagement angle may vary even if the cutting width is kept constant. Hence it is important to generate HSM tool paths with controlled engagement angle.

Our Contribution:

As in our previous work [3], we generate paths for pocketing such that the maximum engagement angle does not exceed a user-specified value. However, by resorting to spiral-like paths (rather than to trochoidal paths) we try to avoid that stages with and without any material removal alternate frequently when our scheme is applied to pockets that are common in practice. It can be expected that this feature makes our approach better applicable to high-speed machining. In addition, our approach allows to respect a user-specified maximum cutting width. It is applicable to arbitrarily shaped pockets without islands.

Circular Disk as Pocket:

We start by examining suitable tool paths for disk-shaped pockets. Then we will extend our strategy to cope with arbitrarily shaped pockets. The goal is to come up with a spiral-like path such that the (disk-shaped) pocket is fully machined when a tool centered on the path is moved from its start point to its end point. Spiral-like means that the path is a continuous trajectory that winds around some central point C several times while progressively receding from it. A *lap* of such a path is a portion of the path that makes one full 360° turn around C. The last lap of our spiral-like paths will be formed by

© 2026 U-turn Press LLC, http://www.cad-conference.net

(a) Tool engagement angle (b) Cutting width

Fig. 1: Illustration of the tool engagement angle θ and the cutting width ν at the same point T along the tool path (shown in purple). The green disk depicts the tool. The blue curves stand for the boundary between the area machined and the area not yet machined (that is indicated by the blue hatching).

an (inwards) offset curve of the pocket boundary. The offset distance r_O is given by $r_O := r + \varepsilon$, i.e, by the radius r of the tool plus some user-specified fudge factor $\varepsilon \geq 0$ used to leave some material uncut for the finishing pass after the last lap of the roughing operation. The laps are numbered and denoted by $\ell_1, \ldots, \ell_n$, for some integer n, with ℓ_n being the last (outermost) lap along the pocket boundary.

All laps wind around C in a counter-clockwise (CCW) fashion. We assume that machining proceeds outwards, from some region around C towards the boundary. This region is assumed to be free of material, e.g., due to pre-drilling or due to a plunging move of the tool along a helical trajectory. Thus, the innermost lap of the tool is given by a circle. It would be easy to modify our approach such that the spiral winds around C in a clockwise (CW) fashion, or to start the machining along the boundary and move the tool inwards. In particular, both up-cut and down-cut machining could be accommodated.

Each lap is split into two circular arcs: One upward arc and one downward arc. Both arcs are semi-circles that make a CCW turn of 180°. We construct the laps and their individual semi-circles from the outermost lap ℓ_n inwards towards ℓ_1. Let θ denote the user-specified threshold on the maximum engagement angle. Suppose that the tool (with radius r) moves along a circular arc with radius r_p. Thus, the boundary of the area left unmachined is a circular arc with the same center and radius $r_p + r$, see Figure 2(a). How deeply may the tool be immersed into the material such that the engagement angle does not exceed θ? That is, for a center position T of the tool, how can we model the point E_θ on the tool such that the angle $\angle(E_\theta, T, L)$ equals θ? If the contact arc of the tool with the material would exceed the CCW arc from L to E_θ then the engagement angle for tool position T would exceed θ.

The point E_θ traces out a curve as the tool center T moves. We call this curve the *envelope of maximal engagement*. Moving T along a circular arc (with center C) causes E_θ to move also along a circular arc whose center lies at C. Our work [3] on trochoidal machining tells us that the radius r_θ of this arc can be computed by applying the law of cosines, see Figure 2(b). By setting $\alpha := 180 - \theta$ we get

$$r_\theta^2 = r^2 + r_p^2 - 2 \cdot r \cdot r_p \cdot \cos\alpha. \tag{2.1}$$

Figure 2c shows a tool (with center T) traversing along a circular arc with center C_1. If the contact arc of the tool with the material is given by the CCW arc from L to E, then the engagement angle for position T is given by $\angle(E, T, L)$. This angle is supposed to be less than or at most equal to θ. A strict inequality holds if E is outside of the circle that corresponds to the envelope of maximal engagement. We have equality if E coincides with E_θ. If the boundary of the area not yet machined is (locally) given by a circle with center C_0 then equality occurs if the point E and the centers C_0 and C_1 are collinear. Thus, a maximum permissible engagement happens exactly if the envelope of maximum engagement touches the boundary of the area not yet machined.

We know that the last lap ℓ_n is given by a full circle. The radii of its upward arc and its downward arc are trivial to compute: If the circle of the pocket disk has radius ρ, then the radius r_p of the last trivial

© 2026 U-turn Press LLC, http://www.cad-conference.net

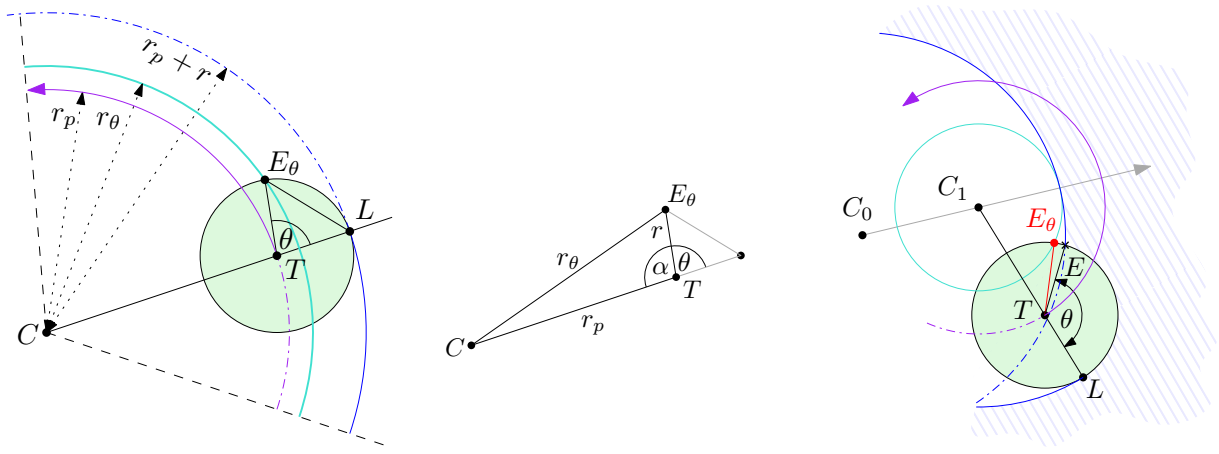

(a) (b) (c)

Fig. 2: The turquoise arc in (a) is the envelope of maximal engagement. It is the trace of the point E_θ as the center T of the tool moves along a circle (in purple) with radius r_p and center C. The blue curve shows the boundary of the area not yet machined. In (b), the relevant geometric entities are extracted. In (c), the point E_θ resides on the envelope of maximal engagement, and point E lies on the machined contour.

lap ℓ_n is given by $r_p = \rho - r_O$, where r_O is the sum of the tool radius r and some user-specified fudge factor. Then it suffices to remember Equation (2.1) to obtain the radius of the circle that models the envelope of maximal engagement for the last lap. Remember that we construct the laps inwards, starting with ℓ_n and obtaining a suitable lap ℓ_{n-1} from it. Then lap ℓ_{n-2} is obtained relative to lap ℓ_{n-1}, and so on; cf. Figure 3. Hence, we have to ensure that machining along lap ℓ_{n-1} removes enough material such that the tool can later on move along the last lap ℓ_n without exceeding θ.

The end point of the downwards arc of ℓ_{n-1} has to match the point S_2. As we try to maximize the amount of material removed within the constraints imposed by θ, we place the start point S_3 of ℓ_{n-1} at a distance of r vertically below the point Y_{max}. The center C_2 of this arc is the middle point between S_2 and S_3, see Figure 3b. Similarly, the start point S_4 of the upward arc of ℓ_{n-1} sits at a distance of r vertically above the point Y_{min}. It is easy to see that this construction ensures that the maximum engagement angle θ is not exceeded when machining along ℓ_n. After all, the dashed envelope of maximal engagement is tangent but does not protrude beyond the area machined by ℓ_{n-1} (and all previous laps).

The same scheme is applied to the construction of lap ℓ_{n-2} relative to lap ℓ_{n-1}. We repeat this construction until an upwards or downwards arc in the spiral reaches a radius less than a user-specified threshold. Depending on the user's preference, at this point in time we either construct a trivial first lap ℓ_1 or stop the spiral path. The actual size of ℓ_1 is application-dependent and, thus, of no concern to us.

Generalization to Arbitrarily Shaped Pockets:

We assume that the pocket $\mathcal{P}$ does not contain islands. Its boundary $\partial\mathcal{P}$ shall be formed by one simple and closed curve that consists of straight-line segments and circular arcs. Let $\partial\mathcal{P}$ be oriented CCW. As in [3], we assume that $\mathcal{P}$ is machinable, i.e., that all material within $\mathcal{P}$ can be removed without gouging.

The key geometric data structure used by our algorithm is the Voronoi diagram $\mathcal{VD}(\partial\mathcal{P})$ of $\partial\mathcal{P}$, together with its sibling, the medial axis $\mathcal{MA}(\partial\mathcal{P})$ of $\partial\mathcal{P}$. For a thorough discussion of the theory, computation, and application of Voronoi diagrams and medial axes of straight-line segments and circular

© 2026 U-turn Press LLC, http://www.cad-conference.net

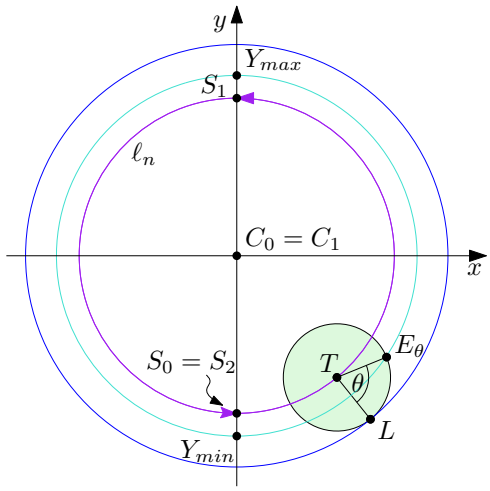

(a) The last trivial lap ℓ_n is displayed with the envelope of maximal engagement (turquoise), machined contour (blue) and tool path (purple).

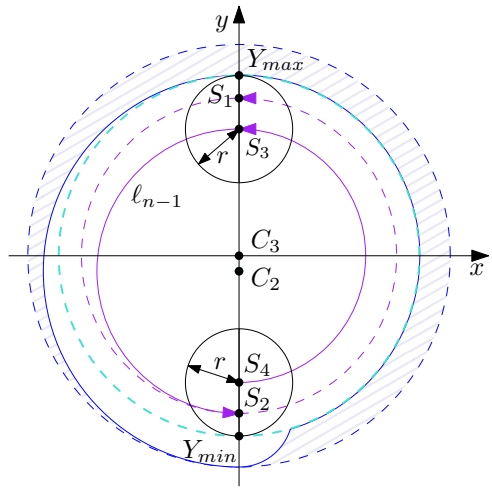

(b) The geometric entities of the lap ℓ_{n-1} relative to ℓ_n are shown. The material remaining uncut after ℓ_{n-1} was fully traversed by the tool is hatched. Dashed are the entities of (a).

Fig. 3: Illustration of the construction of the laps in an inwards manner.

arcs we refer the interested reader to literature on Voronoi diagrams; see, e.g., [2] and its references.

Consider a point P in $\mathcal{P}$ and denote its minimum distance to $\partial\mathcal{P}$ by r_p. Then a disk with radius r_p is the largest-radius disk that can be centered at P such that it is fully contained in $\mathcal{P}$. This disk is known as the *clearance disk* d_p of P, and its radius r_p is called the *clearance distance*. If the clearance disk of P touches $\partial\mathcal{P}$ at point F, then F is called a *foot point* of P, and the straight-line segment $\overline{PF}$ is called a *clearance line*. A point P in $\mathcal{P}$ that has the largest clearance distance among all points of $\mathcal{P}$ is the center of a so-called *maximum inscribed circle* (MIC). Theory tells us at least one node of $\mathcal{MA}(\partial\mathcal{P})$ is the center of a MIC. And this node is easy to determine by scanning $\mathcal{MA}(\partial\mathcal{P})$. See Figure 4a.

Note that $\mathcal{P}$ being machinable implies that all interior points of $\mathcal{P}$ that have a clearance distance of r_O form one (closed) curve. This curve $\mathcal{C}$ is the offset curve of $\partial\mathcal{P}$ for offset r_O. It consists of straight-line segments and circular arcs and is G^1-continuous. It is easy to derive $\mathcal{C}$ on the basis of $\mathcal{VD}(\partial\mathcal{P})$.

The basic idea for handling a general pocket is to start the material removal by constructing a spiral inside the MIC, as explained above. The result for our sample pocket is shown in Figure 4b. As soon as machining within the MIC is finished, the so-called *divergence* process starts. Recall that the last trivial lap is given by a full circle centered at the center of the MIC, and the boundary of the area machined corresponds to the MIC. We generate duplicates of C and let them travel away from C along $\mathcal{MA}(\partial\mathcal{P})$. At appropriate points in time, portions of their clearance disks, together with portions of $\partial\mathcal{P}$, will define the boundary of the area machined so far. The corresponding elements of the tool path are given by circular arcs centered on $\mathcal{MA}(\partial\mathcal{P})$ together with transition segments between them. One can visualize the divergence as an expanding and stretching of the machining contour such that the MIC is morphed to $\partial\mathcal{P}$. This expansion is shown in Figure 5. The final result is shown in Figure 6a.

Now regard $\mathcal{MA}(\partial\mathcal{P})$ as a tree $\mathcal{T}$ rooted at C. Every duplicate stops traveling once it has reached a leaf of $\mathcal{T}$. While other duplicates keep traveling towards the leaves of $\mathcal{T}$, that duplicate remains at its leaf for the rest of the divergence process. The divergence stops once all duplicates have reached their leaves. We conclude the description of the divergence process by explaining how the halting positions

© 2026 U-turn Press LLC, http://www.cad-conference.net

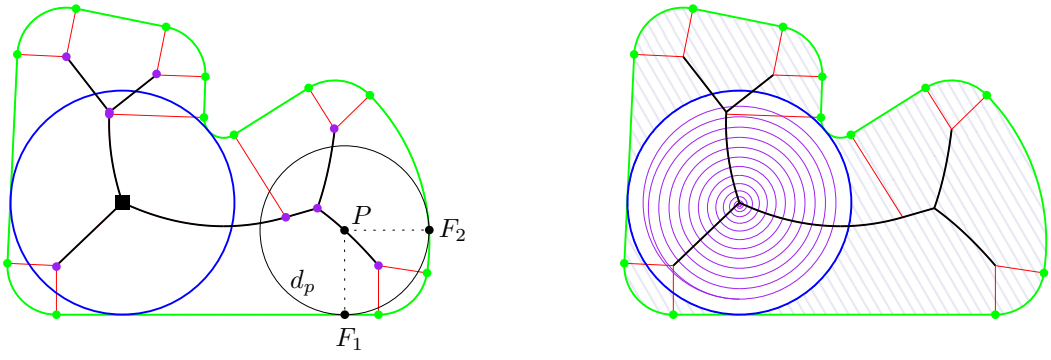

(a) (b)

Fig. 4: The black curve segments in (a) depict the medial axis of the (green) pocket boundary; the black curve segments and the red straight-line segments form its Voronoi diagram. The nodes of the medial axis are indicated by purple disks. A maximum inscribed circle is shown in blue. The clearance disk d_p of point P and its two foot points F_1 and F_2 are given in black; the two clearance lines are dotted. In (b), a sample spiral tool path inside the MIC is shown.

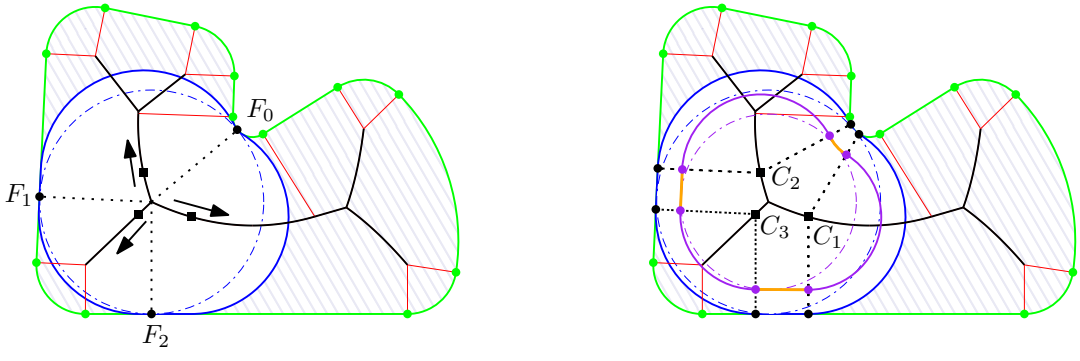

(a) (b)

Fig. 5: Visualization of the divergence process relative to the MIC (blue, dot-dashed). In (a), the initial directions of divergence are indicated by three black arrows. In (b), we see the first lap outside of the MIC: It is composed of three circular arcs (in purple) induced by the clearance disks of the three points (on the medial axis, indicated by black squares) and the transitions along the offset curve $\mathcal{C}$ of $\partial\mathcal{P}$ (in orange) between the respective clearance lines. The last lap inside the MIC is shown in purple dot-dashed.

of the duplicates of C are determined. We employ a strategy similar to the one used in [3] to control the engagement angle: A circular arc of a new lap can be pushed away from its previous lap only so far that the engagement angle does not exceed θ. For a specific position C_1 of the arc's center this requirement holds if the envelope of maximal engagement is nested inside the area machined by the previous lap. Equation (2.1) implies that $r_p + r > r_\theta$ holds if $0° < \theta < 180°$. We know that the maximal tool engagement angle happens if the envelope of maximal engagement is tangent to the corresponding circular arc of the boundary of the area machined; recall Figure 2c. Let C_0 denote the center of that arc.

© 2026 U-turn Press LLC, http://www.cad-conference.net

Then we can move C_1 as far as the following inequality holds:

$$\|C_0 - C_1\| \leq r_p + r - r_\theta \tag{2.2}$$

As in [3], we use Inequality 2.2 as a predicate in combination with a binary search to move C_1 along $\mathcal{MA}(\partial\mathcal{P})$. Figure 6a shows the resulting spiral-like path inside and outside of the MIC.

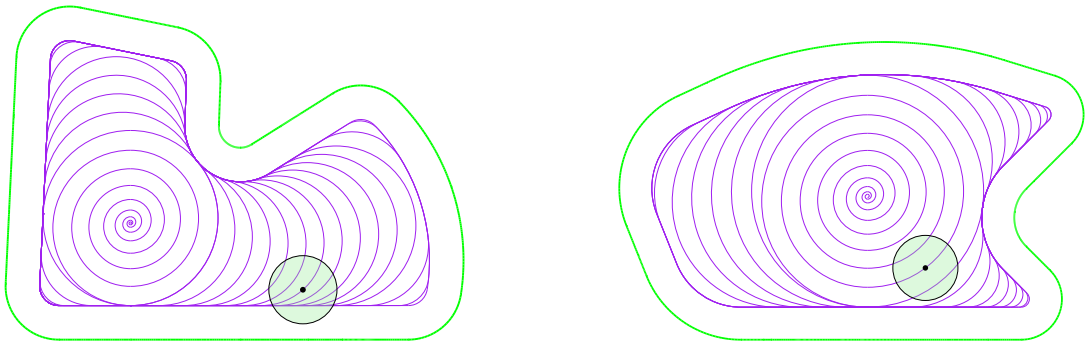

(a) (b)

Fig. 6: Sample tool paths. The green disk represents the tool.

Conclusions:

We implemented our algorithm in C++. Voronoi diagrams and medial axes are computed by means of VRONI/ARCVRONI [2]. On an Intel i7-6700 CPU (clocked at 3.40 GHz) it takes less than 10 milliseconds to compute the Voronoi diagrams and the tool paths for the pockets shown in Figure 6.

The approach outlined above allows to generate $\mathcal{G}^1$-continuous spiral-like tool paths such that a user-specified maximum tool engagement angle θ is not exceeded. It is easy to extend our approach such that both θ and a user-specified maximum cutting width ν are respected. Our algorithm will then vary the cutting width dynamically such that both bounds are respected. Experiments indicate that our approach is particularly better than an approach based on restricting the cutting width for pockets bounded by circular arcs that have significantly different radii.

Martin Held, https://orcid.org/0000-0003-0728-7545
Josef Pfeiffer, https://orcid.org/0009-0003-7865-782X

References:

[1] Elber, G.; Cohen, E.; Drake, S.: MATHSM: Medial Axis Transform toward High Speed Machining of Pockets. Comput. Aided Design, 37(2), 241–250, 2005. https://doi.org/10.1016/j.cad.2004.05.008.

[2] Held, M.; Huber, S.: Topology-Oriented Incremental Computation of Voronoi Diagrams of Circular Arcs and Straight-Line Segments. Comput. Aided Design, 41(5), 327–338, 2009. https://doi.org/10.1016/j.cad.2008.08.004.

[3] Held, M.; Pfeiffer, J.: Trochoidal Tool Paths for Pocket Machining with Full Control of the Tool Engagement Angle. Comput. Aided Design & Appl., 731–747, 2025. https://doi.org/10.14733/cadaps.2025.731-747.

© 2026 U-turn Press LLC, http://www.cad-conference.net